Proceedings of the XVIII ECSMGE 2024
GEOTECHNICAL ENGINEERING CHALLENGES
TO MEET CURRENT AND EMERGING NEEDS OF SOCIETY

ISBN 978-1-032-54816-6
DOI 10.1201/9781003431749-604

ECSMGE 24
XVIII EUROPEAN CONFERENCE ON SOIL MECHANICS AND GEOTECHNICAL ENGINEERING

Modelling hysteretic damping of soils for monopiles

Modélisation de l'amortissement hystérétique des sols pour les monopieux

A.R. Leon Bal*, M. Jafari, L.A. Berenguer Todo Bom, M. Goodarzi
COWI A/S, Hamburg, Germany

*arbl@cowi.com

ABSTRACT: This paper proposes a new method to evaluate the hysteretic soil damping in offshore wind turbines (OWT) with monopiles. Soil damping is a key factor affecting the design of OWT and its fatigue life span. Dynamic 3D finite element analyses incorporating the Hardening Soil-small model are performed. The OWT damping is obtained from the decay of tower displacements. Depending on the expected monopile deflections and soil stiffness, it is found that the widely adopted Cook and Vandiver (1982) method from the oil and gas industry, can underestimate the soil hysteretic damping.

RÉSUMÉ: Cet article propose une nouvelle méthode pour évaluer l'amortissement hystérétique du sol dans les éoliennes offshore (OWT) avec des monopieux. L'amortissement du sol est un facteur clé qui affecte la conception de l'éolienne et sa durée de vie en fatigue. Des analyses dynamiques par éléments finis en 3D intégrant le modèle Hardening Soil-small ont été réalisées. L'amortissement de l'OWT est obtenu à partir de la décroissance des déplacements de la tour. En fonction des déflexions attendues du monopieu et de la rigidité du sol, on constate que la méthode Cook et Vandiver (1982), largement adoptée dans l'industrie pétrolière et gazière, peut sous-estimer l'amortissement hystérétique du sol.

Keywords: Soil damping; offshore wind turbines; finite element analyses; hardening soil model; decay test.

1 INTRODUCTION

The impact of damping in the performance of offshore wind turbines with monopile foundations cannot be understated, as it helps in the reduction of peak displacements of the structure, steel quantities and costs (Versteijlen et al., 2011) and the extension of its life span (Malekjafarin et al., 2022). Therefore, accurate representation of the soil-structure interaction is crucial for the achievement of optimized designs.

Although different damping sources affecting the dynamic response of OWT have been identified, namely, aerodynamic, hydrodynamic, structural and foundation damping, foundation damping remains as one of the major contributors (Malekjafarin et al., 2022). Foundation damping includes radiation, seepage, and hysteretic components, where the soil hysteretic damping is more relevant for OWT and will be the focus of this paper.

2 METHOLOGY

A series of dynamic 3D finite element analyses (FEA) were conducted with Plaxis 3D. The tower geometry in terms of the outer diameter (OD) and wall thickness is also shown in Figure 1 (left). The model setup as well as the FE mesh are shown in Figure 1 (right). Viscous absorbing boundary conditions are used to model the energy dissipation into the far field (radiation damping). The tower was modelled as linear elastic using plate elements. The Rotor-Nacelle Assembly (RNA) was modelled using a rigid circular plate with a fictive density at the tower top to give a mass of 809 tons. Half symmetry in the fore-aft direction was also employed to reduce the model size and hence, the simulations time. The soil behaviour was captured with the Hardening Soil model with small strain stiffness (HS-small). The soil properties are presented in Table 1. Due to the expected low levels of pile deformations under fatigue limit state conditions, the stress dependency of the stiffness parameters of the HS-small model are ignored.

Table 1. Soil parameters of the numerical model.

Unit	Depth [m]	γ_{sat} [kN/m3]	γ_{70} [-]	G_0 [MPa]	E_{50} [MPa]	*Eur [MPa]
A	0-2	19	1.37E-04	25.1	8.6	25.6
B	2-16	19.6	3.90E-04	76.7	22.8	68.4
C	16-49	19.4	3.23E-04	234	41.6	125

*G_{ur} was computed based on E_{ur} and assuming a Poisson's ratio of $\nu = 0.25$.

As discussed in Brinkgreve et al. (2007), the γ_{70} parameter in HS-small is calibrated so that the Plaxis damping ratio curve agrees well with the resonant column test results. The HS-small model employs a shear strain-dependent reduction curve for the shear modulus, which allows for the development of hysteresis loops but yields zero hysteretic damping at very small strains. However, resonant column tests in general show a certain amount of damping even at very small strain levels. Such damping cannot be captured using HS-small model. As a result, Rayleigh damping is often added to the finite element models. Resonant column tests of the soil units in Table 1 indicate that a Rayleigh damping ratio amounting to 1.5% should be added to get a better match of the Plaxis soil damping curves to that of the lab tests. The Raleigh damping coefficients are set to α = 0.01257 and β = 0.01592. These set of parameters result in a Raleigh damping of 1.5% at the natural frequency of the structure (0.17 Hz). Nevertheless, the authors found that the contribution of the Rayleigh damping is negligible due to the extremely low natural frequency of the structure (below 0.2 Hz) and resulting low tower velocity during the structural vibrations.

To observe the free lateral vibrations of the tower in the first mode, the tower head is displaced from the initial position (x = 0 m) to one side (e.g., x = 0.25 m) in a static phase. Then, the tower head is released in a dynamic phase and allowed to vibrate freely. The total duration of dynamic phase is 100 seconds with a step size 0.4 seconds. Several dynamic analyses with different initial lateral displacements (x = 0, 0.5, 1 and 1.5 m) are considered.

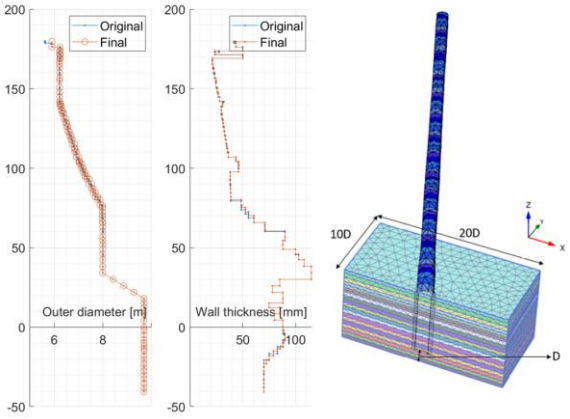

Figure 1. FE model in Plaxis: (left) Final geometry of the tower and pile and (right) FE mesh and soil layering. Very short cans are merged in the final geometry.

3 RESULTS AND DISCUSSION

Time histories of the computed displacement at the mudline for maximum displacements in x-direction of u_{max} = 1.14, 2.34, 5.17 and 8.70 mm are depicted in Figure 2 (left), considering various initial cycle amplitudes at tower top (A_0 = 0, 0.5, 1 and 1.5 m).

A Fast Fourier Transform (FFT) was also performed to extract the frequency content of the displacement time history at the tower head. As seen in Figure 2 (right), the FFT reveals that the natural frequency of the modelled structure is 0.17 Hz.

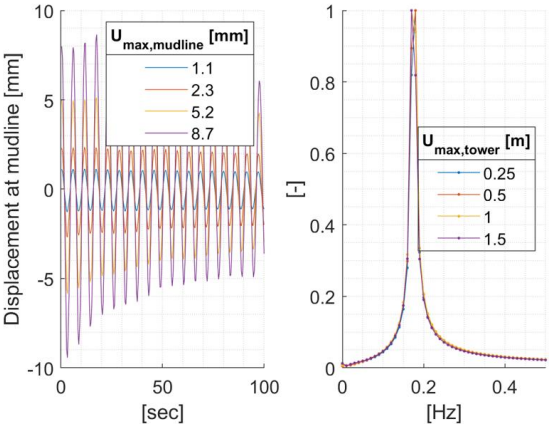

Figure 2. Computed time history of the displacement at the (left) mudline and (right) Fast Fourier Transform of the tower top displacement.

From each displacement time history, cycle peaks are extracted to evaluate the decay of the displacement amplitude. In order to obtain a representative damping ratio coefficient ζ (%) of the system, an exponential decay function $u(t) = A_0 e^{-\zeta 2\pi f_n t}$ is fitted to the extracted cycle peaks of the tower top in which t (s) is the time, A_0 (m) is the displacement amplitude at t = 0 (s) and f_n (Hz) is the natural frequency of the system. The fitted curves can be seen in Figure 3 (left). The back-calculated damping ratios are plotted against the initial mudline displacement in Figure 3 (right).

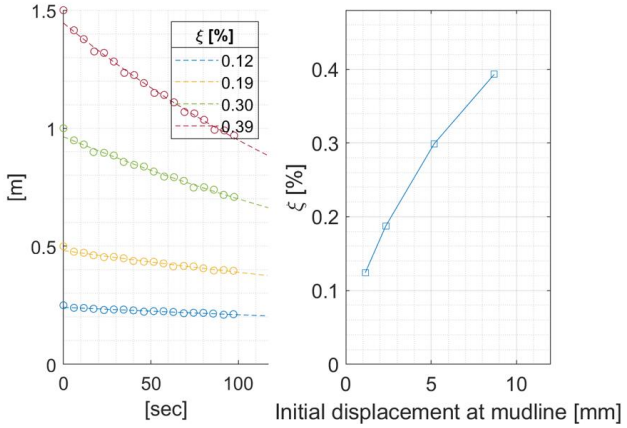

Figure 3. Fitting the exponential decay function to the tower head displacement to find the soil hysteretic damping: (left) Source data from Plaxis and (right) fitted ζ values for the selected cycle amplitudes (0.25, 0.50, 1, and 1.5 m) in correlation to the initial mudline displacement.

The FE-based damping ratio values are compared against those computed using the Cook and Vandiver method (Cook and Vandiver, 1982) for the first vibration mode of the structure. In this method, the pile is discretized into n nodes to which soil reaction springs are connected. The damping ratio ζ is calculated as

$$\zeta = \frac{1}{\omega_n^2 M}\sum_{i=1}^{n} K_s(z_i)\Psi_i(z_i)\zeta_{smd}(z_i) \quad (1)$$

in which $\omega_n = 2\pi f_n$ is the circular natural frequency, M is the modal mass of the structure, $K_s(z_i)$ is the soil spring stiffness for node i at depth z_i, $\Psi_i(z_i)$ is the mode shape of the node for the first deformation mode and $\zeta_{smd}(z_i)$ is the specific soil damping.

The first mode shape and modal mass are obtained by conducting an eigen frequency analysis of the structure, for which the soil interaction springs are extracted from the FE model at every meter along the embedded pile length. The $\zeta_{smd}(z_i)$ is interpolated from the calibrated damping ratio versus shear strain curve, considering the shear strain γ calculated after (Skempton, 1951)

$$\gamma = \frac{1+\upsilon}{2.5\,OD}\cdot y(z_i) \quad (2)$$

in which υ is the soil Poisson's ratio, and $y(z_i)$ is the lateral monopile deflection at z_i computed from a static push-over analysis of a 1-D beam model of the monopile. The soil stiffness K_s is calculated assuming two scenarios:

- K_s is taken as the initial stiffness of the soil reaction springs.
- K_s is taken as a linearized secant stiffness of the soil springs. The linearization level is determined by a static push-over analysis of the 1-D beam model of the monopile, where the mudline is laterally pushed to a certain amount u_{max}. For the analyses u_{max} = 1.14, 2.34, 5.17 and 8.70 mm.

Figure 4 displays the calculated damping ratio as a function of the normalized initial mudline displacement (u_{max}/OD = 0.01, 0.02, 0.05 and 0.09%) considering the two scenarios for the calculation of the soil spring stiffness. In general, the FE-based and the Cook and Vandiver method compares well up to u_{max}/OD = 0.02%, beyond which the Cook and Vandiver method underestimates the soil damping. Therefore, using the secant soil spring stiffness in the Cook & Vandiver method results in very conservative damping ratios. However, taking K_s as the initial stiffness of the springs, a plateau is reached with increasing u_{max}/OD. A plateau indicates that the maximum damping ratio for all the soil damping curves for each node along the monopile has been reached.

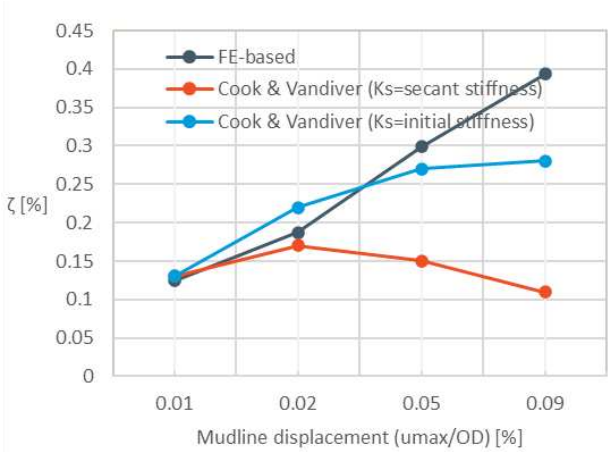

Figure 4. Damping ratio vs. maximum normalized mudline displacements according to (Cook and Vandiver, 1982) and FE calculations.

The increase of damping ratio values with increasing amplitudes of cyclic loading has been also reported in the literature (Malekjafarin et al., 2022). The Cook and Vandiver method, on the other hand, cannot capture this increasing trend properly due to the following factors:

- Utilization of the soil secant stiffness K_s instead of the stiffer loading/unloading K_{ur} stiffness. The stiffness. K_{ur} is more representative of the soil behaviour. For fatigue limit state conditions where pile displacements are very low, K_{ur} is relatively close to the initial stiffness of the springs (K_{ini}). As the mudline displacement increases, the secant stiffness reduces. This reduction is more pronounced for large u_{max}/OD ratios and does not compensate the increase in specific damping ratio ζ_{smd} with increasing strains, leading to an overall decrease of the soil damping ratio.
- Inherent uncertainties in the calculation of shear strains from pile displacements. The correct estimation of the soil shear strains is of paramount importance for the accurate determination of the specific damping ratio and in turn, the soil hysteretic damping.
- The influence of the pile diameter. While the Cook and Vandiver formulation was calibrated and tested against typical pile foundations in the oil and gas industry decades ago, current monopiles with smaller length to diameter ratios behave more rigidly, exhibiting a different deformation mode characterized by rotations along the shaft as well as rotations and lateral

displacements along the base (Burd et al., 2020). By extending Eq. (1) with additional rotational and pile base terms (e.g., rotational stiffness, modal rotations, etc.), more realistic hysteretic damping values could be attained.

4 CONCLUSIONS

In this contribution, a new FE-based methodology based on a free vibration analysis of the wind turbine structure is presented for the estimation of hysteretic soil damping in OWT's. The FE-based damping ratio is compared with that of the Cook and Vandiver methodology. The utilization of the Cook & Vandiver method can result in an underestimation of the hysteretic soil damping depending on the expected monopile deflections and the assumed soil stiffness in its formulation. The main characteristics of the proposed numerical strategy are the following:

- A 3D FE model comprising the tower, monopile and the rotor nacelle assembly.
- The incorporation of the Hardening Soil model with small strain stiffness, capable of reproducing hysteresis loops in the soil via the strain-driven degradation of the small-strain shear modulus.
- Performing dynamic analysis as part of numerical decay tests with selected initial cycle amplitudes at the tower top.
- The generation of damping curves (for each cycle amplitude) from the tower peak displacements and the subsequent exponential fitting to extract the damping ratio.
- Transforming tower displacements to mudline displacements and finding the damping ratio at the desired mudline displacement from the resulting damping ratio-mudline displacement curve.

For the assessed mudline displacements, the proposed methodology consistently predicted increasing damping ratios for increasing cycle amplitudes. To have a baseline, results computed with the Cook and Vandiver method were presented. Results from this method but using instead the secant soil stiffness calculated from the smallest cycle amplitude were also included. For larger mudline displacements, the Cook and Vandiver method failed to capture the positive correlation between cycle amplitudes and damping ratios. On the other hand, by using the soil secant stiffness from the smallest cycle amplitude (u_{max}/OD = 0.01), the gap with the FE-based results was substantially reduced.

Finally, the utilization of the secant or the initial soil spring stiffness, the transformation from pile displacements to soil shear strains and the pile diameter, were identified as potential factors hindering the accuracy of the Cook and Vandiver method for large mudline displacements.

REFERENCES

Brinkgreve, R. B. J., Kappert, M. H. and Bonnier, P. G., (2007). Hysteretic damping in a small-strain stiffness model. In: *Proc. of Num. Mod. in Geome*ch., NUMOG X, Rhodes, Greece, pp. 737-742.

Burd, H. J., Taborda, D. M., Zdravković, L., Abadie, C. N., Byrne, B. W., Houlsby, G. T., ... and Potts, D. M. (2020). PISA design model for monopiles for offshore wind turbines: application to a marine sand. *Géotechnique*, 70(11), pp. 1048-1066, https://doi.org/10.1680/jgeot.18.P.277.

Cook, M. F., and Vandiver, J. K. (1982). Measured and predicted dynamic response of a single pile platform to random wave excitation. In: *Offshore Technology Conference (OTC)*, Houston, Texas, USA, pp. 637-643., https://doi.org/10.4043/4285-MS.

Malekjafarian, A., Jalilvand, S., Doherty, P., and Igoe, D. (2021). Foundation damping for monopile supported offshore wind turbines: A review. *Marine Structures*, 77(102937), pp. 1-22, https://doi.org/10.1016/j.marstruc.2021.102937.

Skempton, A.W., (1951). The bearing capacity of clays. *Selected papers on soil mechanics*, pp. 50-59., https://doi.org/10.1680/sposm.02050.0008.

Versteijlen, W. G., Metrikine, A., Hoving, J. S., Smid, E., and De Vries, W. E. (2011). Estimation of the vibration decrement of an offshore wind turbine support structure caused by its interaction with soil. In: *Proceedings of the EWEA offshore 2011 conference*, Amsterdam, The Netherlands.